Available online at www.sciencedirect.com
SCIENCE DIRECT
Polymer 46 (2005) 11849–11857
polymer
www.elsevier.com/locate/polymer

Polyurethane elastomers through multi-hydrogen-bonded association of dendritic structures

Chih-Ping Chen [a], Shenghong A. Dai [a,*], Huey-Ling Chang [b], Wen-Chiung Su [c], Tzong-Ming Wu [d], Ru-Jong Jeng [a,*]

[a] *Department of Chemical Engineering, National Chung Hsing University, Taichung 402, Taiwan, ROC*
[b] *Department of Chemical Engineering, National Chinyi Institute of Technology, Taichung 411, Taiwan, ROC*
[c] *Chung-Shan Institute of Science and Technology, Lungtan, Tauyuan 325, Taiwan, ROC*
[d] *Department of Material Engineering, National Chung Hsing University, Taichung 402, Taiwan, ROC*

Received 31 October 2004; received in revised form 18 June 2005; accepted 25 June 2005
Available online 26 October 2005

Abstract

A series of hydrogen bonding-rich polyurea/malonamide dendrons have been utilized as building blocks for the synthesis of novel dendritic polyurethane elastomers. Based on the resulting microstructure of soft segments reinforced by the rigid dendritic domains, the hydrogen bonding enforced phase separation of segmented polyurethanes was explored. DSC and FT-IR results indicate that a certain degree of phase separation between dendritic and poly(tetramethylene oxide) (PTMO) domains. The domain size of phase separation are less than 100 nm based on the results obtained from the atomic force microscopy (AFM) and small-angle X-ray scattering (SAXS). The analysis of tensile measurements indicates that the incorporation of various contents of different dendrons as the hard segments allows these polymers to exhibit drastically different mechanical properties. Furthermore, low complex viscosity is observed at medium temperatures (above 130 °C) via the rheological analysis. With good mechanical properties at room temperature and low melt viscosity at medium temperatures, these thermoplastic elastomeric polyurethanes are suitable for applying in hot-melt process.

Keywords: Dendrimer; Hydrogen bond; Polyurethane

1. Introduction

Self-assembly is a very efficient way of building large or complicated structures which would be otherwise complex and time-consuming to synthesize directly by the covalent synthesis [1,2]. In supramolecular polymers, for instance, rational engineering of crystal lattices successfully leads to novel electric, magnetic, molecular encapsulation or thermally reversible materials [3–5]. Many researches concerning about the use of the secondary force to build the advanced materials, which are expected to be highly advantageous over traditional polymers because of their tunable and reversible characteristics. Such materials, however, are very rare even in the polymer systems. Researchers [6–8] have made a detailed study of the effect of hydrogen bonding groups aggregate in a cooperative fashion to form thermoplastic elastomers. Furthermore, Meijer and co-workers described the strong dimerization of 2-ureido-4[1H]-pyrimidinones by quadruple hydrogen bonding and the formation of linear thermal-reversible polymers [8,4]. Recently, Hamachi and co-workers [9] used glycosylated amino acid to prepare the supramolecular material, which was capable of acting as a carrier matrix for the thermally controlled release of DNA. In those cases, the association of functional groups via a certain interaction leads to the formation of supramolecular domains serving as physical crosslinks, which result in materials with much improved properties.

Dendrimer and hyperbranched polymers have aroused great interests lately, because of their potential applications such as drug delivery agents, catalysts, hybrid systems, and nano-technologies [10,11]. This is because the presence of numerous end groups in these dendritic polymers. For example, an unique copolymers with core-shell architectures or a highly cross-linked network can be acquired via the incorporation of dendritic structures. Recently, a series of convergent polyurea/malonamide dendrons were developed in our laboratory [12]. Based on sequential selective addition

* Corresponding authors. Tel.: +886 4 228 52581; fax: +886 4 228 54734.
E-mail address: rjjeng@dragon.nchu.edu.tw (R.-J. Jeng).

0032-3861/$ - see front matter © 2005 Elsevier Ltd. All rights reserved.
doi:10.1016/j.polymer.2005.06.127

reactions of isocyanato-azetidine-2,4-diones, rapid entry into polyurea/malonamide dendrons was achieved via the convergent route with the processing advantages of easy purification, high yield and rapid synthesis. The chemical structures of these dendrons are shown in Fig. 1. A secondary amine is present at the focal point for each dendron. Moreover, different contents of urea and amide linkages are present in inward section and periphery depending on the size of the dendron. These hydrogen bonding-rich groups provide diversified associated chains, which would be the ideal candidates for the formation of supramolecular structures. It is important to note that the urea-rich groups not only provide additional hydrogen-bonding sites, but inter-urea bonds are also capable of forming stronger hydrogen-bonding linkages with three-dimensional characteristics [13–16]. Keeping these in minds, the goal of this study is to explore the hydrogen bonding enforced phase separation of segmented polyurethanes by incorporating these well-defined, regular and hydrogen bonding-rich structures as the association units. Since, the early work of Cooper and Tobolsky [17], it has been established that multi-block copolymers composed of hard and soft segments are generally microphase-separated into high-T_g

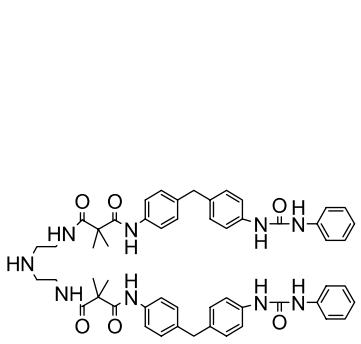

[G-1]-NH

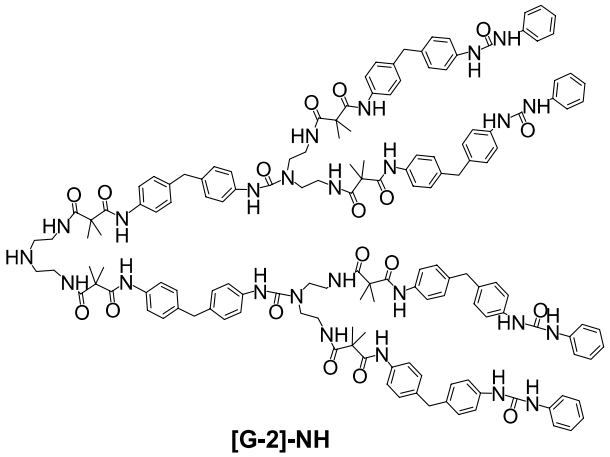

[G-2]-NH

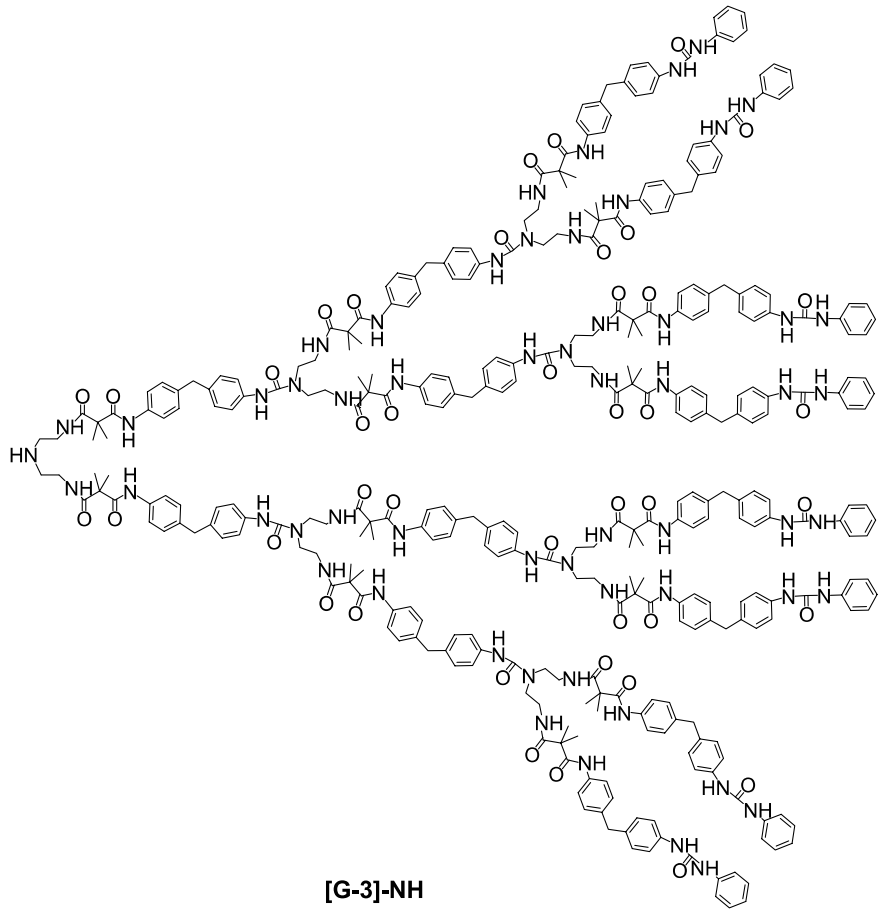

[G-3]-NH

Fig. 1. Chemical structures of [G-1]-NH, [G-2]-NH and [G-3]-NH polyurea/malonamide dendrons.

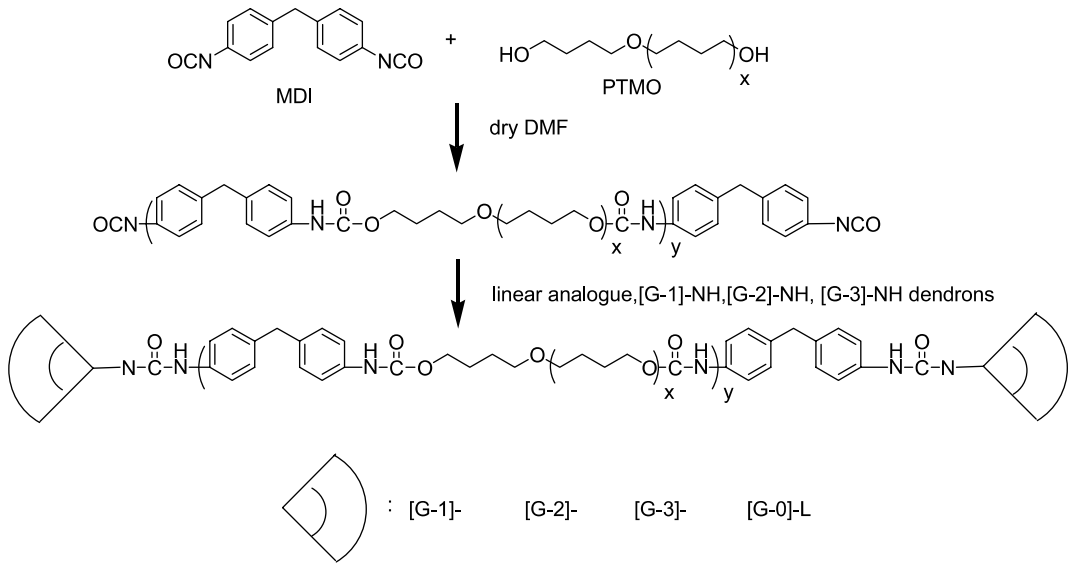

Fig. 2. Preparation of dendritic polyurethane elastomers via hydrogen-bonded rich structures.

(hard; sometimes crystalline) domains and relatively low-T_g (soft) domains. The resulting microstructure of soft segments reinforced by rigid hard domains exhibits excellent elastomeric properties, making these polymers useful as elastomers, textiles, coatings, biomaterials, etc. [18–20]. Herein we present a unique type of the polyurethane elastomers, by incorporating the linear analogue or dendritic structures as the end-capped hard segments, and the poly(tetramethylene oxide) glycol (PTMO) as soft segments. Moreover, to show the versatility of this approach, these dendrons were reacted with different ratios of the 4,4′-methylene di(*p*-phenyl isocyanate) (MDI) to PTMO (Fig. 2). On the basis of experimental results obtained from thermal analysis, morphological study, and tensile measurements, the present paper describes the effect of dendrons on hydrogen bonding induced phase separation and mechanical properties of the dendritic polyurethane elastomers. Furthermore, the rheological behavior was investigated.

2. Experimental parts

2.1. Synthesis of linear analogue([G-0]-L; Scheme 1)

[G-0]-A was synthesized according to the literature (Scheme 1) [12]. To a solution of [G-0]-A (5 g, 12.1 mmol) in dry DMF (50 ml) aminoethyl piperazine (1.56 g, 12.1 mmol) was added. The solution was stirred at 30 °C under a nitrogen atmosphere for 2 h. The resulting solution was poured into water, filtered and washed with acetone. Then the product was dried under the reduced pressure at 70 °C for 12 h to give a 6.04 g of white solid. The yield was 92%.

IR (KBr): 3325 (NH), 1653 cm^{-1} (*C*=*O* (NH)).

^1H NMR (DMSO-d_6): $\delta = 1.38$ (s, 6H, $C(CH_3)_2CONH$), 2.60 (t, 10H, CH_2–NH), 3.13 (t, 2H, CH_2–NHCO), 3.80 (s, 2H, Ar–CH_2–Ar), 6.90–7.60 (m, 13H, Ar–H).

($C_{31}H_{38}N_6O_3$) (542): Calcd C 68.61, H7.06, N 15.49; Found C 69.03, H6.84, N 15.09.

2.2. Synthesis of dendritic polyurethane elastomers

Several dendritic polyurethane elastomers with different compositions were synthesized via a two-step condensation reaction. The reactions were carried out in a solution of dry dimethylformamide (DMF) using a 2000 g/mol PTMO, end-capped with MDI and then adding the linear analogue([G-0]-L) or dendrons ([G-1]-NH, [G-2]-NH and [G-3]-NH dendrons). The PTMO, MDI and DMF were purchased from Aldrich Chemical, Co. PTMO was degassed by vacuum pump before use. For detailed information regarding dendrons ([G-1]-NH, [G-2]-NH and [G-3]-NH dendrons) and synthetic procedure, one can refer to our previous publication [12]. PTMO (5 wt%) was dissolved in DMF and stirred in a flask while freshly distilled MDI was added to the solution. These two reactants were heated to 80 °C and remained at this temperature for 2 h. The reaction was cooled to 60 °C before the dendron or [G-0]-L was added. The dendron or [G-0]-L was diluted in DMF

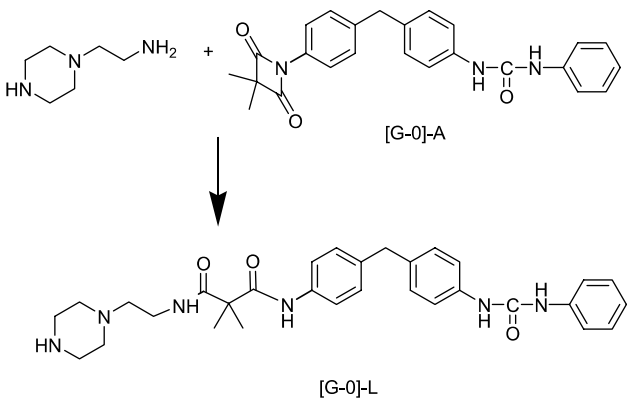

Scheme 1. Synthesis of linear analogue [G-0]-L.

and dripped into the stirring reaction. The reactions were then stirred for approximately 2 h to give series of polyurethane elastomers.

All of these dendritic polyurethane elastomers are identified by 'DXPXXX', the first number denoting to the generation of dendron, the follow numbers denoting to the molar ratio among MDI, PTMO and dendron. MDI and dendron units are assigned to be the hard segment [20]. Hard segment weight fraction is then obtained from the total weight of the elastomer divided by the hard segment weight. The polyurethane elastomer end-capped with [G-0]-L is identified by LP212 with a hard segment content of 44.1%.

2.3. Sample preparation

Samples were prepared as the following. The as-polymerized solutions (~10 wt%) were poured into Teflon circular disks and placed under vacuum at room temperature for 24 h. The oven temperature was then raised to 70 °C and maintained at this temperature for an additional 24 h. Films were on the order of 5 mm thick. Samples of all series copolymers were prepared using this approach.

2.4. Instrumentation

Thermal analysis was performed in N_2 on a TA Instruments DSC2010 at a heating rate of 10 °C/min under a N_2 atmosphere. The samples were initially annealed at 200 °C for 10 min to clear all previous thermal history. The glass transition temperatures (T_g) were determined from the first heating runs, after the cooling rate of 10 °C/min from 200 to −100 °C. For the endotherms the transition temperature was taken at the maximum of the peak and the peak for the glass transition at the midpoint. Thermogravimetric analysis was performed by a Seiko SSC-5200 thermogravimetric analyzer (TGA) at a heating rate of 10 °C/min under nitrogen. Thermal degradation temperature (T_d) is taken at 5% weight loss. Dynamic mechanical thermal analyses were recorded on a TA Model 2940 dynamic mechanical analyzer (DMA). Measurements were carried out at a frequency of 1 Hz and heating rate of 2 °C/min. IR measurements were performed on a Perkin–Elmer Spectrum One FT-IR spectrometer. The morphology of the polymer films was also analyzed by atomic force microscopy (AFM; Seiko SPI3800N, Series SPA-400) with the dynamic force mode at ambient temperature. An etched Si probe under resonant frequency of 139 kHz and spring constants of 16 N/m was used. Small-angle X-ray scattering (SAXS) measurements were performed in transmission mode using a 18 kW Rigaku D/MAX-2500 equipped with Ni-filtered CuKα radiation in the transmission mode. A one-dimensional SAXS data were recorded on a 1D SC-70 Scintillation Counter. The sample to detector distance was ~40 cm and the momentum transfer vector (q, nm^{-1}) is defined as $q=(4\pi/\lambda)\sin(\theta/2)$, where λ and θ are the wavelength and the scattering angle, respectively. Tensile measurements were carried out on specimens having a dimension of 5 mm wide and 20 mm length using a Shimadzu testing machine with a cross-head speed of 50 mm/min at room temperature. Dynamic mechanical measurements were carried out with a Rheometrics RDA2 in the oscillatory mode in parallel-plate geometry (25 mm). The disc gap of the rheometer was 0.7 mm. A fixed strain of 0.06 was used to ensure that measurements were taken well within the linear viscoelastic range of the materials studied.

3. Results and discussion

Recently, we presented the synthesis of polyurea/malonamide dendron([G-1]-NH, [G-2]-NH, and [G-3]-NH) (Fig. 1) [12]. The present study extends the previous investigation to develop polyurethane elastomer via incorporating these dendritic structures. Furthermore, a linear analogue ([G-0]-L) (Scheme 1) was synthesized to compare with these dendritic materials. The polymerization was carried out via a two-step condensation reaction to give a series of polyurethanes [21,22] (Fig. 2). In the first step, the isocyanate terminated precursor was obtained. Then the amino containing dendritic structure was added. Base on the high reactivity between the amine and isocyanate, the reaction was completed instantly [21]. IR spectrum was used to confirm the formation of polyurethanes with the characteristic absorption peak of NCO (2260 cm^{-1}) as an index to determine the degree of reaction. Appearances of the dendritic polyurethanes were either transparent or milky opaque (Table 1).

3.1. Thermal properties of the dendritic polyurethanes

The thermal stability of dendritic polyurethane was investigated by TGA analysis. Thermal properties of these dendritic polyurethanes are shown in Table 1. All the polymers exhibited their T_ds higher than 260 °C. No weight loss was observed for these polymers within the temperature range of 30–240 °C. DSC was utilized to understand the phase separation behaviors of these dendritic polymers. The same thermal protocol was used in our DSC study. The samples were heated at 200 °C for 10 min in order to erase all previous thermal histories. The transition temperatures were then determined from the first heating runs, after the cooling rate of 10 °C/min from 200 to −100 °C. Fig. 3 shows the DSC thermograms of the D1P322 and D2P432 samples. There are three transitions in each thermogram including a T_g(s) of soft segment, a melting point of the crystalline soft segment, T_m, and a hard segment transition temperature (T_g(h)). According to Seymour and Cooper's studies [23,24], the high temperature endotherms transitions (i.e. T_g(h)) may attributed by phase-segregated structures of the long range ordering of hard-segment domains. For these polymers, a soft-segment T_g(s) of −50 to −65 °C and a T_m around 20 °C were observed, which are substantially different from those of the pristine PTMO [25]. Based on these criteria, this indicates that a certain degree of mixing between hard- and soft-segment was present in the polymers. In one example, it has been clearly established that the phase mixing would increase the T_g of the PTMO soft segment in PU elastomers. It important to note that the T_g of the pristine PTMO sample is around −80 °C [25]. In addition,

Table 1
Physical properties of dendritic polyurethane elastomers

Sample	H_c[a]	A	T_d[b] (°C)	T_g[c] (°C)	T_m[d] (°C)	T_g[e] (°C)	T_b[f] (MPa)	ε_b[g] (%)	E[h] (MPa)	q_{max}[i] (nm^{-1})	d_i[j] (nm)
D1P212	50	T	260	−56	24	139	4.5	196	57	0.180	35
D1P322	39.5	T	288	−57	21	132	5.0	952	11	0.160	39
D1P432	32.3	O	312	−58	23	132	N/A[k]	N/A	N/A	N/A	N/A
LP212	44.1	T	283	−54	23	123	1.0	140	12	0.12	52
D2P432	50.8	T	279	−57	22	120	0.7	37	38	0.095	66
D2P652	40.1	T	265	−60	21	117	4.0	696	6	0.100	63
D2P762	36.7	O	297	−58	21	125	0.2	1000	1	N/A	N/A
D2P12112	41.2	O	310	−54	25	140	2.5	120	19	N/A	N/A

A, appearance; T, transparency; O, opaque.
[a] Hard segment content (wt%).
[b] Five percent weight loss.
[c] Glass transition temperature of soft segment.
[d] Melting point of soft segment.
[e] Glass transition temperature of hard segment.
[f] Tensile strength at break.
[g] Elongation at break.
[h] Young's modulus.
[i] The q value at maximum intensity of $I(q)$ vs q plot.
[j] Interdomain distance between soft phase domains.
[k] D1P432 is incapable of forming film due to its gummy physical form at room temperature.

the observation of the presence of three thermal transitions can be used as an indication of a distinct phase-separated morphology. Moreover, the absence of re-crystallization peak of PTMO during heating scan indicates that the soft segment can be completely crystallized with a previous cooling scan of 10 °C/min. This implies the presence of a phase-separated structure with each phase being composed of a rich phase [26].

3.2. FT-IR analysis

FT-IR spectroscopy has been proven to be a useful instrument for the investigation of hard-soft segment interactions in many phase-separated copolymers [13–16]. This technique was used in the present study to estimate the phase-separation in the dendritic polyurethanes and to examine changes in degree of hydrogen bonding which is temperature-dependent. FT-IR spectra of D1P322 and D2P652 at 30 °C are shown in Fig. 4. The CH_{asym} and CH_{sym} stretching vibration peaks of the PTMO soft segments are located at 2939 and 2854 cm^{-1}, respectively. The NH stretching vibration from 3299 to 3314 cm^{-1}, and the carbonyl stretching vibration from 1600 to 1800 cm^{-1} are contributed by the urethane, urea and amide linkages. Of particular interest are the absorption band characteristics of urethane carbonyl stretching peaks. All spectra appear to be composed of two bands at the urethane carbonyl stretching region. The band centered around 1731 cm^{-1} is assigned to stretching of free urethane carbonyl groups, while the band at 1709 cm^{-1} is attributed to hydrogen-bonded urethane carbonyl groups [14,15]. These frequencies would shift to values lower than those observed when these groups are free. In this case, there are many NH proton donors within the dendritic polyurethanes including urea, amide and urethane linkages. The presence of two absorption characteristics for the proton acceptor, carbonyl oxygen of the urethane groups indicates that the hydrogen-bond disruption occurs either at domain interfaces or when phase mixing of the hard and soft segments takes place [15]. This leads to a certain degree of phase separation between dendritic and PTMO domains. Because of the immiscibility between the dendritic and PTMO segments, these polymers undergo microphase separation. Normally the ratio of these two peaks can be used as 'hydrogen bonding index' to estimate the extent of hydrogen bonding. However, it is hard to quantitatively determine the degree of phase separation via Gaussian function of FT-IR analysis due to the structure complexity (i.e. the presence of urea, urethane, and amide linkages) between soft and hard segments in this work.

Further investigation of the phase separation behavior was performed by IR spectra at various temperatures. Fig. 5 shows the IR spectra of the urea and urethane carbonyl stretching region heating from 30 to 200 °C for the D1P322. In the spectrum at 30 °C, the urethane carbonyl stretching vibration exhibits a board absorption peak centered at around 1710 cm^{-1}

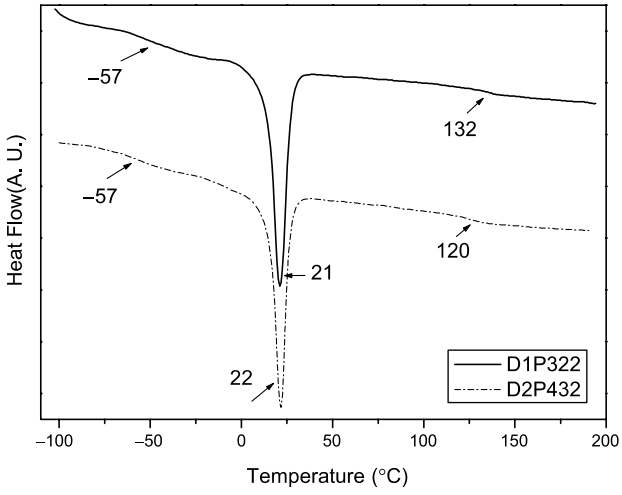

Fig. 3. DSC thermogram of D1P322 and D2P432 samples.

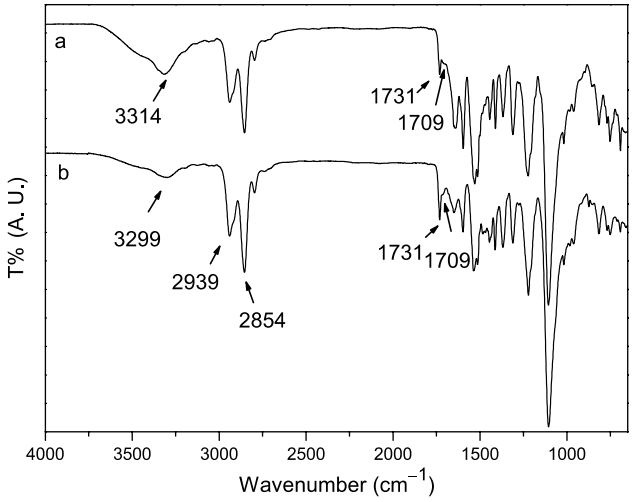

Fig. 4. FT-IR spectra of (a) D1P322 and (b) D2P652 samples.

mainly arising from the hydrogen bonding of NH (urea, amide or urethane) to carbonyl groups (urethane), while the free carbonyl stretching vibration appears at about 1730 cm^{-1}. As temperature is increased, the intensity of the hydrogen-bonded carbonyl stretching band decreases, and the peak position is continuously shifted toward a higher wavenumber. This implies that the initial hydrogen bonding of the N–H proton donors in D1P322 is weakened with increasing temperature, resulting in an increased population of free urethane carbonyl groups. Similar tendency is also observed for the stretching vibration band of hydrogen-bonded urea or amide carbonyl at 1650 cm^{-1}, which shifts to higher wavenumber as the temperature is increased from 30 to 200 °C. The number of free urea carbonyl groups increases with increasing temperature, whereas the number of the hydrogen-bonded groups does otherwise. This also indicates that the microphase separation structure will become homogenous when the temperature increases. Based on the above, it is important to note that the hydrogen-bonding linkages via urethane carbonyl functional groups show the initial dissociation above 90 °C, and nearly disappear at the temperatures above 130 °C. As will be discussed in the following section, the hydrogen-bonding dissociation of urethane carbonyl groups result in the low complex viscosity behaviors of dendritic polyurethanes.

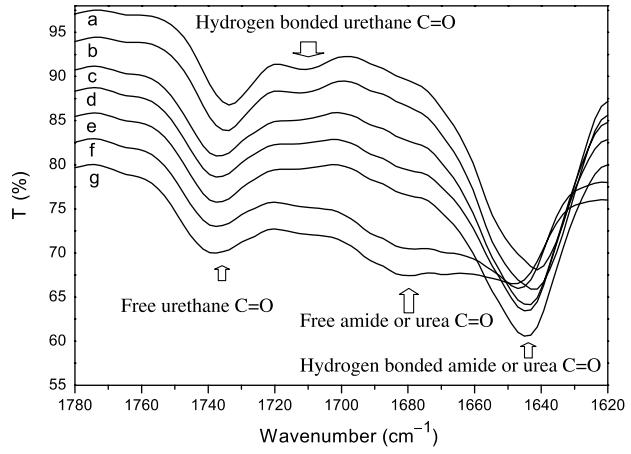

Fig. 5. IR spectra of the carbonyl stretching region for the D1P322 sample at various temperature. (a) 30 °C; (b) 90 °C; (c) 130 °C; (d) 160 °C; (e) 170 °C; (f) 180 °C; (g) 200 °C.

3.3. Morphology

From above DSC results, the dendritic polyurethanes show a melting temperature at about 20 °C which is corresponding to the crystalline PTMO phase. Therefore, the dendritic polyurethanes contain two phases morphology composed of amorphous PTMO phase (disordered structure) and hydrogen-bonding rich dendron domain (ordered structure) at room temperature. The small-angle X-ray scattering (SAXS) and atomic force microscopy (AFM) experiments were utilized to investigate the microphase-separated morphology of dendritic polyurethanes at room temperature. According to scattering curves ($I(q)$ vs q) obtained by SAXS, the peak position and scattering intensities can provide the characteristic of microphase-separated morphology [27,28]. The explanation of SAXS data for multi-phase systems is a complex function of the structure and the arrangement of different scattering phases. However, the interpretation of a single scattering peak in a SAXS curve can be only observed for a specific structure and regular arrangement. In our case, the microphase-separated morphology of this novel polymer may differentiate from several end-capping agent choices to various contents of hard segments. For the ease of interpretation of SAXS data, the lamellar architecture of dendritic polyurethanes is assumed for this study [27]. As shown in Fig. 6, the SAXS curve for the D1P322 sample is presented. The maximum intensity at $q_{max} = 0.16\ nm^{-1}$ can be observed in the scattering curve. According to this data, a rough estimation of the average interdomain distance (d_i) between soft-phase domains can be obtained from the peak position of the peak maximum (q_{max}) through the Bragg equation [25,26]:

$$d_i = \frac{2\pi}{q_{max}}$$

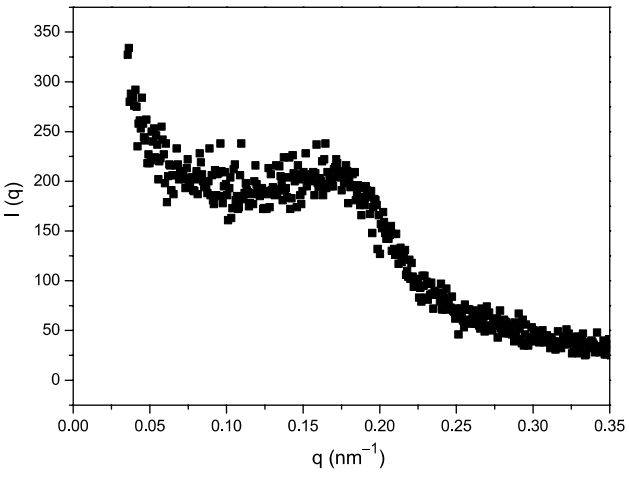

Fig. 6. SAXS intensity as a function of scattering vector for D1P322 sample.

After calculation, $d_i = 39$ nm is obtained. Similar results are also obtained for other systems. Moreover, the average interdomain distances between soft-phase domains are presented in Table 1. As a result of SAXS interpenetration, there are certain amounts of ordered structures observed for these microphase-separated dendritic polyurethanes, which are under the scale of 100 nm.

To shed the light on the microphase separation, AFM experiments were conducted in a separate study on all series of dendritic polyurethanes. According to the study of Karbach et al. [29,30], the AFM dynamic force mode phase images can provide information for understanding morphological features between hard and soft segments. Fig. 7 shows the AFM result of the cast 'surface' of D1P322 including topography image, phase image, and cross-sectional image on the line. Obviously, ordered microphase separation is present for the D1P322 sample. On the phase image (Fig. 7(b)), the hard domains appear to be the bright regions, whereas the dark regions denote to the soft segments [18,29,30]. The irregular soft spherical domains were randomly distributed with lateral dimensions in the order of approximately 50 nm in the polymer matrices. As shown in Fig. 7(c), the cross-sectional phase image on the line for the D1P322 sample can be utilized to estimate the distance between the separate microphase domains. The interdomain spacing between two soft domains is approximately 45 nm which is consistent with the data obtained by SAXS analysis.

3.4. Mechanical and rheological properties

Dynamic mechanical analysis provides information on microphase separation, glass transition and the mechanical properties of dendritic polyurethanes. Fig. 8 shows the variations of the storage modulus and tan δ with temperatures for two samples with the same hard segment content differing in the type of end-capping agents. Well-defined peaks in tan δ at about -50 °C were observed in both samples which corresponded to the glass transition temperatures of amorphous domains of soft segments from the DSC results. At this particular temperature range, a drop in modulus about three orders in magnitude was observed. Moreover, a rubbery plateau around 10×10^6 Pa was discernible between -30 and 20 °C for D1P322. Obviously, the material exhibits the characteristics of an elastomer at room temperature [31]. As compared to non-dendritic PTMO-MDI polymers, the remarkable improvement of mechanical properties indicates that the dendritic structures play a major role via inducing hydrogen bonding microphase separation, i.e. interchain interactions such as physical crosslinks are present. As the temperature further increased, the hydrogen-bonding induced polymer became more viscous liquid-likes. Consequently, the modulus drops drastically. A sharp peak in tan δ and well-defined plateau in E' above the soft-segment glass transition indicate that materials are microphase-separated [32]. The thermal and dynamic mechanical behavior of LP212 based on DMA analysis is qualitatively similar to that of the D1P322 sample, but in a somewhat higher modulus, particularly at the rubbery plateau.

Dynamic oscillatory shear measurement was performed on the D1P322 sample. The frequency dependence of the storage modulus G', loss modulus G'' and complex viscosity at 140 °C is shown in Fig. 9. D1P322 behaved essentially as fluids and exhibited the characteristic of $G'' > G'$ above the dissociation

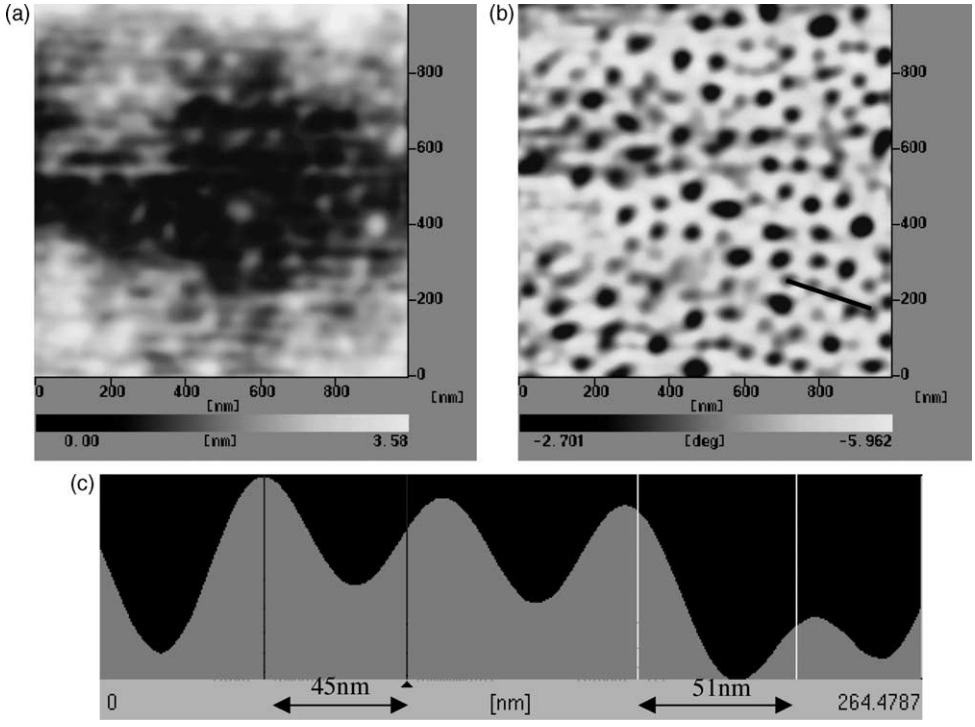

Fig. 7. AFM topography image (a); phase image (b); and cross-sectional image on the line in phase image (c) for the D1P322 sample.

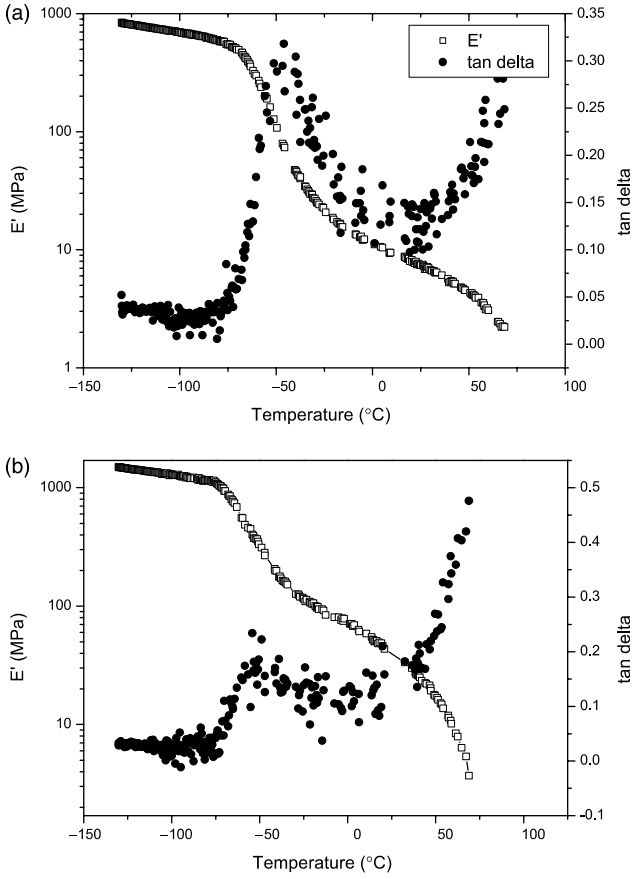

Fig. 8. DMA curves of (a) D1P322 and (b) LP212 samples.

temperature of hydrogen bonding of the urethane carbonyl groups. Moreover, a rather low complex viscosity around 3×10^3 Pa.s and similar frequency-independent complex viscosities behavior at 140 °C were observed. Based on the DMA and rheological results, these thermoplastic elastomeric dendritic polymers possessing good mechanical properties at room temperature and a low melt viscosity at medium temperatures are suitable for applying in hot melt process.

Tensile properties of these dendritic polyurethanes were also analyzed. As shown in Table 1, the elongation properties are composition-dependent. The elongation increased with

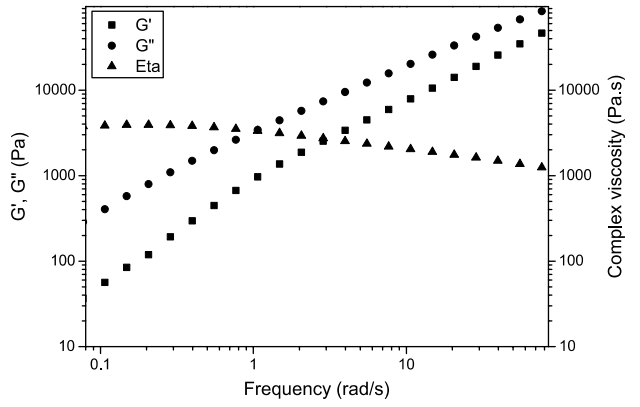

Fig. 9. Storage modulus G', loss modulus G'' and complex viscosity as a function of frequency for D1P322 at 140 °C.

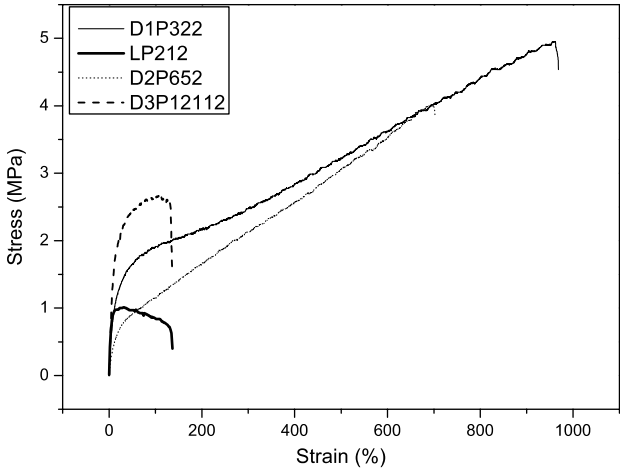

Fig. 10. Stress–Strain behavior of different end-capped dendritic polyurethane elastomers with similar hard segment contents.

increasing content of PTMO, which is in agreement with the elongation properties of the commercial polyurethane elastomers containing various contents of PTMO [33]. Moreover, the modulus was dependent on the hard segment content for the same end-capping dendron system. Fig. 10 shows the stress–strain behavior for four different end-capped dendritic polymers with similar hard segment contents. The D1P322 sample was found to exhibit better mechanical properties with a tensile strength of 5 MPa and an elongation of 952%, despite that LP212, D1P322, D2P652 and D3P12112 consisted of similar hard segment contents, and exhibited similar characteristics by DSC and FT-IR analyses. It is well documented that the properties of segmented PU are strongly dependent on their microphase morphologies [34]. According to literature [33], the opaqueness indicates that the macrophase separation is present between the hard and soft segments for the D3P12112 sample. On the other hand, the microphase separation is present for the transparent LP212, D1P322 and D2P652 samples. Although, the SAXS analysis indicates the LP212, D1P322 and D2P652 have the similar average interdomain around 50 nm. As shown in Fig. 11, the AFM phase images of these optical transparency materials seem to provide interpretation of the differentiation among the mechanical properties of LP212, D1P322, D2P652 and D3P12112. As mentioned in previous section, irregular soft spherical domains were randomly distributed in the order of approximately 50 nm for the D1P322 (Fig. 7), whereas the distinction between light and dark regions appears unclear for LP212 and D2P652 (Fig. 11). Better mechanical properties for D1P322 are possibly due to its well-defined microphase-separated morphology. D1P322 consisting of generation one dendron seems to provide more strong hydrogen bonding, and subsequently leads to exhibit clear boundary between hard segments and PTMO soft segments. It is noteworthy that these dendritic end-capping polyurethanes did not exhibit comparable mechanical properties with the commercial polyurethanes. Commercial polyurethanes are typically made by the reaction of a diisocyanate with polyol and chain extender [21,33]. The chain-extension compounds (short chain diol or diamine) would lengthen the main chain of

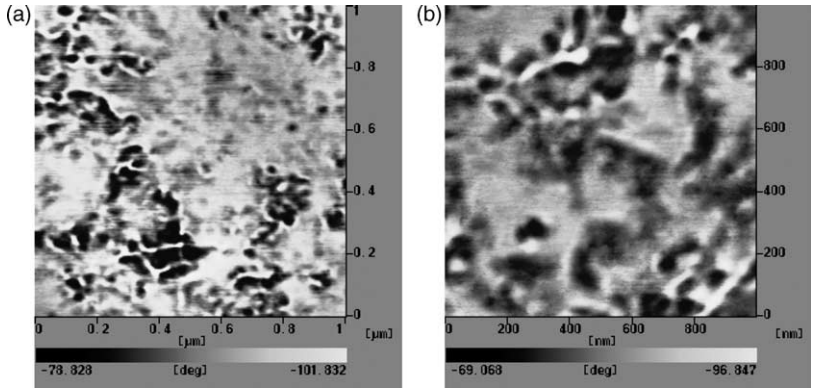

Fig. 11. AFM phase images of (a) LP212 and (b) D2P652 samples.

the isocyanate terminated precursors via end-to-end attachments. Moreover, these chain-extended end-to-end attachments would serve as the hard segments of the polymer structures. The incorporation of these extended hard segments would certainly enhance the mechanical properties of polyurethanes. In this work, these end-capping agents would not lengthen the main chain of the polyurethanes. The dendtitic structures, instead of playing the role of chain extender, simply provide pseudo-crosslinking sites via physical bonding.

4. Conclusion

Hydrogen bond-rich dendritic structure can be used as a building block for synthesizing the high performance advanced materials using reversible physical bonding. DSC, FT-IR, AFM and SAXS results indicate a certain degree of phase separation between dendritic and PTMO domains. Based on the DMA and tensile measurements, these hydrogen bonding-induced microphase separation of the dendritic domains and soft domains allows the materials to possess better mechanical properties.

Acknowledgements

Financial support from National Science Council of Taiwan, ROC (NSC-91-2216-E-005-005) and Chung-Shan Institute of Science and Technology is gratefully acknowledged.

References

[1] Abed S, Boileau S, Bouteiller L. Macromolecules 2000;33:8479.
[2] Cate ATT, Sijbesma RP. Macromol Rapid Commun 2002;23:1094.
[3] Brunsveld L, Folmer BJB, Meijer EW, Sijbesma RP. Chem Rev 2001; 101:4071.
[4] Sijbesma RP, Beijer FH, Brunsveld L, Folmer BJB, Hirschberg JHKK, Lange RFM, et al. Science 1997;278:1601.
[5] Service RF, Szuromi P, Uppenbrink J. Science 2002;295:2395.
[6] Bica CID, Burchard W, Stadler R. Eur Polym J 1997;33:1759.
[7] Muller M, Dardin A, Seidel U, Balsamo V, Ivan B, Spiess HW, et al. Macromolecules 1996;29:2577.
[8] Sijbesma RP, Meijer EW. Chem Commun 2003;5.
[9] Kiyonaka S, Sugiyasu K, Shinkai S, Hamachi I. J Am Chem Soc 2002; 124:10954.
[10] Frechet JMJ. J Polym Sci, Part A: Polym Chem 2003;41:3713.
[11] Tomalia DA, Frechet JMJ. Dendrimers and other dendritic polymers. West Sussex: Wiley; 2001.
[12] Chen CP, Dai SA, Jeng RJ, Su WC, Chang HL. J Polym Sci, Polym Chem 2005;43:682.
[13] Coleman MM, Sobkowiak M, Pehlert GJ, Painter PC. Macromol Chem Phys 1997;198:117.
14 Teo LS, Chen CY, Kuo JF. Macromolecules 1997;30:1793.
[15] Sung CSP, Schneider NS. Macromolecules 1977;10:452.
[16] Rubner MF. Macromolecules 1986;19:2114.
[17] Cooper SL, Tobolsky AV. J Appl Polym Sci 1966;10:1837.
[18] Koberstein JT, Galambos AF, Leung LM. Macromolecules 1992;25: 6195.
[19] Garrett JT, Runt J, Lin JS. Macromolecules 2000;33:6353.
[20] Revenko I, Tang Y, Santerre JP. Surf Sci 2001;491:346.
[21] Ulrich H. Chemistry and technology of isocyanate. New York: Wiley; 1996 p. 103.
[22] Li FG, Liu ZF, Liu XP, Yang XY, Chen SG, An YG, et al. Macromolecules 2005;38:69.
[23] Seymour RW, Cooper SL. Macromolecules 1973;6:48.
[24] Ng HN, Allrgrezza AE, Seymour RW, Cooper SL. Polymer 1973;14: 255.
[25] Hu CB, Ward RS, Schneider NS. J Appl Polym Sci 1982;27:2167.
[26] Kojio K, Fukumaru T, Furukawa M. Macromolecules 2004;3:3287.
[27] Saiani A, Rochas C, Eeckhaut G, Daunch WA, Leenslag JW, Higgins JS. Macromolecules 2004;37:1411.
[28] Garrett JT, Lin JS, Runt J. Macromolecules 2002;35:161.
[29] Karbach A, Drechsler D. Surf Interface Anal 1999;27:401.
[30] Sormana JL, Meredith JC. Macromolecules 2004;37:2186.
[31] Folmer BJB, Sijbesma RP, Versteegen RM, Rijt JAJ, Meijer EW. Adv Mater 2000;12:874.
[32] Velankar S, Cooper SL. Macromolecules 2000;33:395.
[33] Hepburn C. Polyurethane elastomer. 2nd ed. London: Elsevier; 1992.
[34] Yilgor E, Yurtsever E, Yilgor I. Polymer 2002;43:6561.